Author/s:
Wesemann, L;Panchenko, E;Singh, K;Gomez, DE;Davis, TJ;Roberts, A

Title:
Plasmonic Metasurfaces for Optical Information Processing

Date:
2019-01-01

Citation:
Wesemann, L., Panchenko, E., Singh, K., Gomez, D. E., Davis, T. J. & Roberts, A. (2019). Plasmonic Metasurfaces for Optical Information Processing. Simpson, MC (Ed.) Juodkazis, S (Ed.) SPIE MICRO + NANO MATERIALS, DEVICES, AND APPLICATIONS 2019, 11201, SPIE-INT SOC OPTICAL ENGINEERING. https://doi.org/10.1117/12.2539751.

Plasmonic Metasurfaces for Optical Information Processing

L. Wesemann[1]*, E. Panchenko[1], K. Singh[1], D. E. Gomez[2],
T.J. Davis[1] and A. Roberts[1]
[1] School of Physics, The University of Melbourne, 3010, Australia
[2]RMIT-University, Victoria 3000, Australia
*lwesemann@student.unimelb.edu.au

ABSTRACT

Optical spatial frequency filtering is a key method for information processing in biological and technical imaging. While conventional approaches rely on bulky components to access and filter the Fourier plane content of a wavefield, nanophotonic approaches for spatial frequency filtering have recently gained attention. Here computational and experimental progress towards the design and demonstration of metasurfaces with spatial frequency filtering capability for optical image processing will be presented. Using the example of a metasurface consisting of radial rod trimers we demonstrate its potential to perform edge enhancement in an amplitude image and conversion of phase gradients in a wavefield into intensity modulations. The presented results indicate a potential avenue for ultra-compact image processing devices with applications in biological live-cell imaging.

Keywords: Optical Image Processing, Plasmonic Metasurface, Live-cell imaging, Optical Spatial Differentiation

1. INTRODUCTION

Metasurfaces are artificially fabricated, ultrathin films exhibiting a tailored response to incident electromagnetic radiation. The properties of optical wavefields, such as polarization and phase, can be exploited in applications ranging from information processing, communications and imaging. Here we present the utilization of subradiant plasmonic modes, i.e. modes with zero net-dipolar moment, of nanostructures to create metasurfaces that directly filter the spatial frequency content of a wavefield reflected from or transmitted through the metasurface. This is in contrast to traditional all-optical approaches that require a lens to permit access to the Fourier plane for conventional spatial filtering. Hence, subradiant modes provide an avenue for the development of ultracompact devices that will perform on-chip, real-time, single-shot conversion of phase information to readily measured intensity distributions with applications ranging from optical communication, all-optical spatial image differentiation for face-recognition algorithms through to highly specialized live-cell imaging.

2. PLASMONIC METASURFACE AS A SPATIAL FREQUENCY FILTER

Various plasmonic nanostructures have proven to exhibit subradiant characteristics [1, 2]. As an example, Fig. 1 demonstrates the excitation of bright and dark modes of a radial trimer of silver nanorods with an SEM image shown in Fig. 1(a) [3].

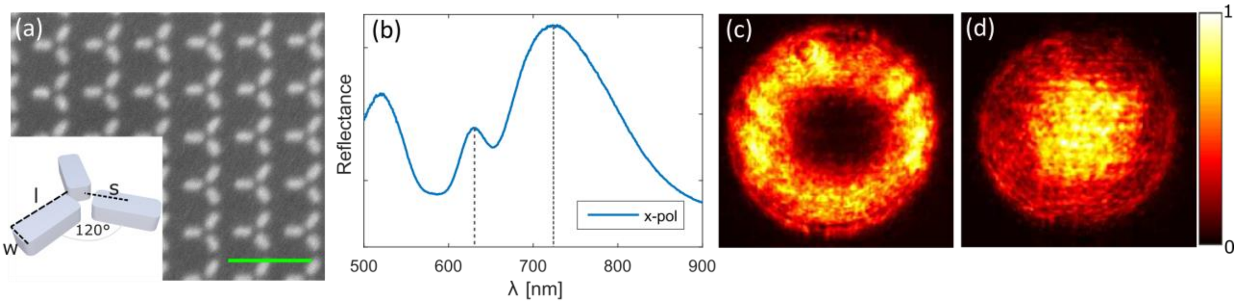

Figure 1. Experimental demonstration of phase sensing capability of plasmonic metasurfaces. a) Scanning electron microscope (SEM) image of device under consideration with inset defining parameters. Scale bar is 500 nm. b) Reflectance spectra of the metasurface and c), d) Fourier plane images at 628 nm and 722 nm respectively.

The lowest energy bright and dark modes have a spectral separation that increases with decreasing rod separation, *s*. Fig. 1(b) shows the reflectance from the array when illuminated with a 0.90 NA objective. Fig. 1 (c) and (d) show the Fourier plane image of the reflected light for x-polarization at 628 nm and 722 nm respectively. The suppression of low spatial frequencies suggests the excitation of a dark mode and an avenue to directly modify the spatial frequency content of an image.

We use this spatial frequency filtering capability of the metasurface to demonstrate numerically and experimentally edge enhancement in an amplitude image reflected from the device. In Fig.2 we demonstrate edge enhancement for the example of a microscopic figure '2' reflected from the metasurface with the amplitude modulation shown in Fig. 2a. In the calculated reflectance from the device shown in Fig.2b enhanced edges are apparent with homogenous regions appearing dark. The corresponding experimental data shown in Fig.2c is in line with the calculated result.

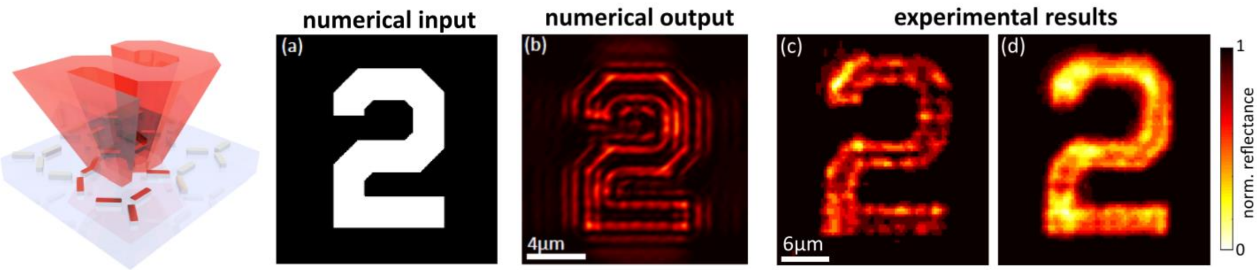

Figure 2. Numerical and experimental demonstration of edge enhancement capability of a radial trimer metasurface. a) Binary input image and b) calculated image reflected from the metasurface at the excitation wavelength of the dark mode (580 nm, s-polarization). c) Experimentally captured image reflected from the metasurface for *x*-polarized illumination at the dark mode wavelength d) Reference image for reflection from the glass substrate. All images are normalized to their brightest pixel.

The capability of the metasurface to detect phase gradients in an incident wavefield is demonstrated numerically in Fig.3. Using COMSOL Multiphysics we have determined the optical transfer function of light reflected from the metasurface. For a wavefield with a Gaussian shaped phase excursion (Fig.3a), the reflected intensity distribution exhibits maxima at locations of high phase gradient, i.e. the slopes of the Gaussian function. This result indicates the potential of the metasurface for phase-imaging of biological cells. Results from the metasurface presented here and related systems including thin film approaches will be discussed.

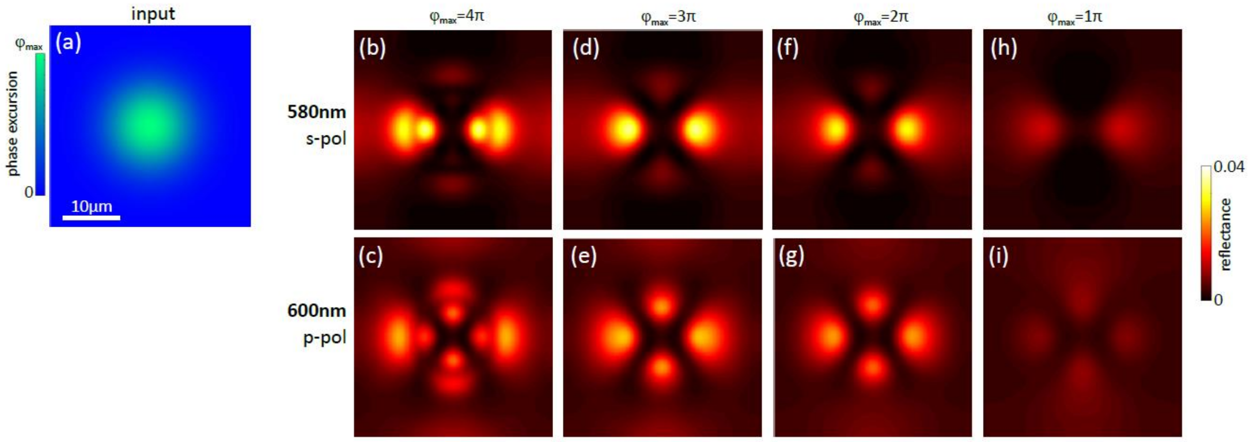

Figure 3. Numerical demonstration of conversion of a phase gradient in an incident wave field into an intensity modulation in the reflected image. a) Gaussian shaped phase modulation incident onto the metasurface b)-i) Reflected Intensity distribution as a fraction of the incident intensity at the excitation wavelengths of the dark modes for different maximum phase excursions and s-polarization (top row) and p-polarization (bottom row).

This work was performed in part at the Melbourne Centre for Nanofabrication (MCN) in the Victorian Node of the Australian National Fabrication Facility (ANFF). This research was also supported under the Australian Research

Council's Discovery Projects funding scheme project number DP160100983. D.G. acknowledges the ARC for support through a Future Fellowship (FT140100514).

REFERENCES

[1] D.E. Gómez, Z.Q. Teo, M. Altissimo, T. J. Davis, S. Earl, and A. Roberts, Nano Lett. 13, 3722-3728 (2013)
[2] F. Hao, P. Nordlander, Y. Sonnefraud, P. Dorpe, and S. A. Maier, ACS Nano 3, 643-652 (2009)
[3] L. Wesemann, P. Achmari, K. Singh, E. Panchenko, T. D. James, D. E. Gómez, T. J. Davis, and A. Roberts, OSA Continuum 1.2, 727-735 (2018)